# Bolometric calibration of a superfluid 3He detector for Dark Matter search: direct measurement of the scintillated energy fraction for neutron, electron and muon events

Clemens Winkelmann, Johannes Elbs, Yuriy M. Bunkov, Eddy Collin, Henri Godfrin, Matti Krusius

# Bolometric calibration of a superfluid $^3$He detector for Dark Matter search: direct measurement of the scintillated energy fraction for neutron, electron and muon events

C. B. Winkelmann [a], J. Elbs [a], Yu. M. Bunkov [a,1], E. Collin [a], H. Godfrin [a], and M. Krusius [b]

[a] *Institut Néel, CNRS and Université Joseph Fourier, BP 166, F-38042 Grenoble Cédex 9, France*

[b] *Low Temperature Laboratory, Helsinki University of Technology, FIN-02015 HUT, Espoo, Finland*

**Abstract**

We report on the calibration of a superfluid $^3$He bolometer developed for the search of non-baryonic Dark Matter. Precise thermometry is achieved by the direct measurement of thermal excitations using Vibrating Wire Resonators (VWRs). The heating pulses for calibration were produced by the direct quantum process of quasiparticle generation by other VWRs present. The bolometric calibration factor is

analyzed as a function of temperature and excitation level of the sensing VWR. The calibration is compared to bolometric measurements of the nuclear neutron capture reaction and heat depositions by cosmic muons and low energy electrons. The comparison allows a quantitative estimation of the ultra-violet scintillation rate of irradiated helium, demonstrating the possibility of efficient electron recoil event rejection.

*Key words:* Dark Matter, Superfluid Helium-3, Bolometer, Scintillation.

*PACS :* 95.35; 67.57; 07.57.K; 11.30.P

---

[1] Corresponding author : yuriy.bunkov@grenoble.cnrs.fr (phone: +33 4-76 88 12 52)

## 1 Introduction

Superfluid $^3$He-B at ultra-low temperatures is an appealing target material for bolometric particle detection [1–3], with complementary features to the currently highest performance germanium- and silicon-based detectors like Edelweiss [4] and CDMS [5]. Among the attractive features of $^3$He are the clear signature of neutron background events due to the nuclear capture reaction of neutrons in $^3$He. Furthermore, the huge density of unpaired neutrons leads to a significantly enhanced axial interaction cross-section within a large class of WIMP models [6,7]. Its single thermal energy reservoir allowing for direct thermometry, the very low experimental base temperature of about $100\,\mu$K, together with the possibility of electron recoil rejection, make $^3$He a very promising target material for Dark Matter search.

The nuclear neutron capture reaction $^3$He+n $\rightarrow^3$ H+p releases 764 keV kinetic energy to its products, and was detected bolometrically in the superfluid [3]. The comparison of the detected neutron peak to bolometric calibrations of the detector was then used [8] as a test of topological defect creation scenarios in fast second order phase transitions [9]. A bolometric calibration method of the detector was first described in [10]. In the following years, the detection threshold of the bolometer could be lowered, which allowed the identification of a broad peak at about 60 keV that could be attributed to cosmic muons, in agreement with numerical predictions. In very recent measurements on a Dark

Matter detector prototype, the detection threshold reached the keV level and the low energy electron emission spectrum from a $^{57}$Co source could be resolved [11,12]. Since the neutralino's interaction with a $^{3}$He nucleus in the detector is expected to deposit a maximum energy of about 5.6 keV, the current detector design therefore already displays the required bolometric sensitivity.

The recent improvement of the sensitivity was partly made possible by lowering the working temperature of the detector cells from about 150 to 130 $\mu$K. This temperature decrease of less than 20% represents a decrease in the thermal enthalpy of the cells by an order of magnitude. On the other hand, at lower temperature the weaker coupling of the VWR to the superfluid results nevertheless in a greater response time of the thermometer. Parallely, the non-linear velocity dependence of the friction with the superfluid [13] is also of greater importance at the lower temperatures and the higher VWR-response signals currently used. This article hence proposes a generalization of the methods described in [10] for a more profound and comprehensive understanding of the bolometric detector (sections 2 to 4) and its calibration by mechanical heater pulses (section 5). The comparison of the bolometric calibration with detection spectra from known energy sources like neutrons (section 6) as well as low energy electrons and muons (section 7) allows then a precise estimation of the ultra-violet (UV) scintillation rate of helium for several types of ionizing radiation.

## 2 Principle of detection

The current $^3$He particle detector [11,12] consists of three adjacent cylindrical copper cells, of volume $V = 0.13$ cm$^3$ each, immersed inside a superfluid $^3$He bath at ultra-low temperature, at about 130 $\mu$K. A 200 $\mu$m diameter orifice in the wall of the cells connects the $^3$He inside the cell with the surrounding heat reservoir of superfluid. An energy deposition by an incident particle creates a cloud of quasiparticles in the cell, which comes to internal thermal equilibrium via collisions on the cell walls within $\sim 1$ ms. The excess ballistic quasiparticles, of momentum $p \approx p_F$, then leak out of the cell with a time constant $\tau_b$ of a few seconds, which is determined mainly by the size of the orifice .

The Vibrating Wire Resonators (VWRs) used for thermometry are thin (4.5 $\mu$m diameter in our setup) superconducting NbTi filaments bent into an approximately semi-circular shape of a few mm, with both ends firmly fixed [14]. The VWR is driven by a Laplace force imposed by an AC current close to its mechanical resonance frequency (≈500 Hz), and oscillates perpendicularly to its main plane with an $rms$ velocity $v$. The motion is damped by frictional forces of total amplitude $F(v)$, mainly due to momentum transfer to the quasiparticles of the surrounding superfluid. Relatively fast thermometry is then achieved by measuring continuously the damping coefficient $W \propto F/v$ of a VWR driven at resonance. In the low oscillation velocity limit, the friction is

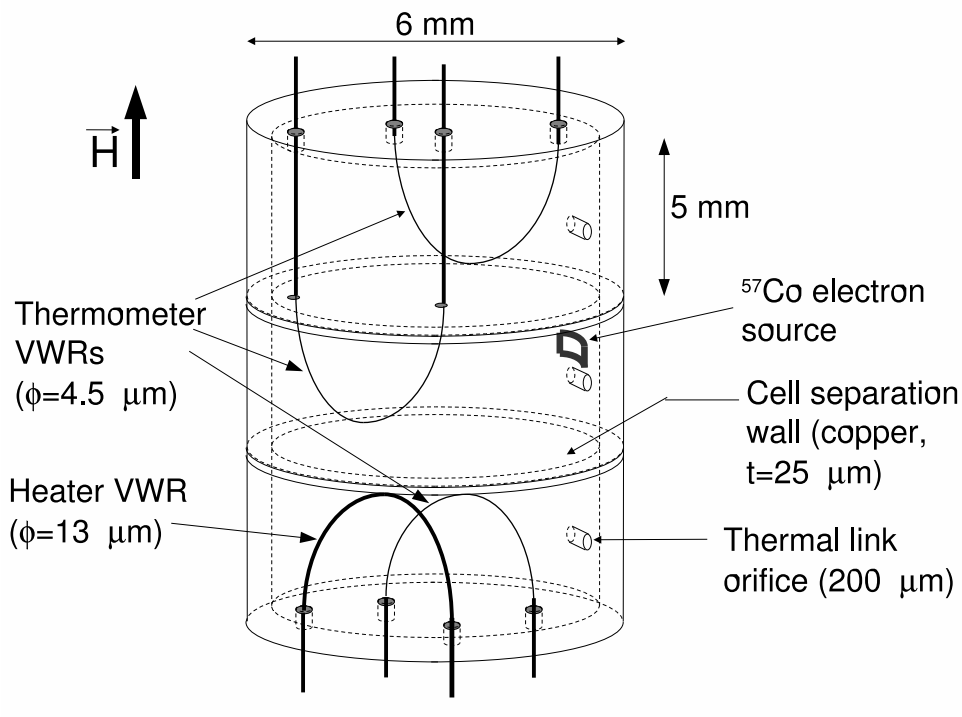


Fig. 1. Schematic setup of the 3-cell bolometric detector prototype. Each cell contains a VWR thermometer. The cells are in weak thermal contact with the outer $^3$He bath through the orifice. The presence of three adjacent cells allows discrimination through coincident detection. One of the cells contains the $^{57}$Co source (section 7), another one contains an extra VWR for the purpose of bolometric calibration by heater pulses (section 5).

of a viscous type $F \propto v$. $W$ is thus velocity independent and can be written as [15]

$$W_0 = \alpha \ \exp(-\Delta/k_B T), \tag{1}$$

where $\Delta$ is the superfluid gap at zero temperature. The value of the prefactor $\alpha$ is determined by both the microscopic properties of the liquid and the geometry of the VWR. At 0 bar and for the VWRs used in the detector, of density $\rho = 6.0$ g/cm$^3$ and radius $a = 2.3$ $\mu$m, $\alpha$ is of the order of 1-2 $10^5$ Hz,

depending on the exact geometrical features. In quasi-static conditions, the low velocity damping coefficient $W_0$ is measured as the Full Width at Half-Height $\Delta f_2$ of the mechanical oscillator's lorentzian resonance in frequency space.

At finite oscillation velocities however, effects beyond the two-fluid model discovered in Lancaster lead to a velocity dependent damping coefficient which is actually decreasing at higher velocities (Fig. 2). A model proposed by Fisher *et al.* [13,15] leads to a velocity dependent damping

$$W_L(v) = W_0 \times L(v/v_0), \tag{2}$$

where the function

$$L(u) = (1 - e^{-u})/u \tag{3}$$

gives a very good approximation of the reduction of the damping of the VWR for $v$ up to a characteristic oscillation velocity $v_0 \sim k_B T/p_F \approx$ 1-2 mm/s.

At higher velocities, of about 3-4 mm/s, the local flow field around sharp edges on the VWR surface starts to get turbulent [16]. At even higher velocities, the critical velocity for pair-breaking is achieved. Both cases correspond to a strong enhancement of the friction, with a strongly non-linear, sometimes even discontinuous, velocity dependence (Fig. 2). While the Lancaster-type non-linear coupling to the superfluid can easily be accounted for by using equation (2), the velocity has thus still to be kept small enough for both the locally turbulent and the pair-breaking regime to be avoided.

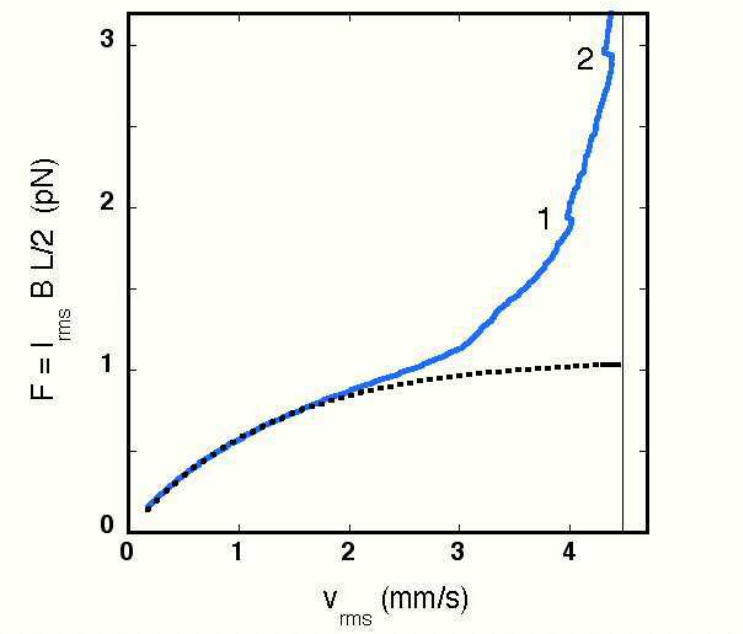


Fig. 2. Isothermal force-velocity ($\equiv (I, V)$) curve of a VWR immersed in superfluid $^3$He at ultra-low temperatures (blue line). For *rms* oscillation velocities below 2 mm/s, the damping is well described by (2)(dashed line). The decrease of the damping coefficient ($\sim F/v$) at higher velocities actually leads to an increase of the calibration factor (section 4). At velocities above about 2.5 mm/s, the slope increases again. Points 1 and 2 show two discontinuities of the force-velocity curve (see text). The friction diverges as the pair-breaking velocity (about 4.5 mm/s) is approached.

## 3 Response of the detector to a heat release

As the quasiparticle density, the temperature and thus $W_0$ as defined by (1) increase nearly instantaneously ($\sim$ 1 ms) after a particle impact, the mechanical VWR only responds to this modification over a timescale inversely

proportional to the dissipative coupling

$$\tau_w = \frac{1}{\pi W_L}. \tag{4}$$

This can therefore result in non-negligible response times (>1 s) for low damping coefficients, i.e. narrow resonances and low temperatures. While recording transitory heating events, the *dynamically* measured damping $W_{mes}(t)$ is thus a non-equilibrium measurement of $W(t)$.

A simple model of a sudden increase of $W$ from its baseline $W_{base}$ by an amount $A \ll W_{base}$ at $t = 0$, and the subsequent exponential relaxation of the quasiparticle excess via the orifice

$$W(t) = W_{base} + A\ e^{-t/\tau_b}\ \Theta(t), \tag{5}$$

leads to a dynamic damping measurement given by

$$W_{mes}(t) = W_{base} + A\frac{\tau_b}{\tau_b - \tau_w}\left[e^{-t/\tau_b} - e^{-t/\tau_w}\right]\Theta(t). \tag{6}$$

$\Theta(t)$ is here the Heaviside function accounting for the instantaneous heat input and since $A$ is a small perturbation, $\tau_w \approx constant = 1/\pi W_{base}$ is assumed. The good agreement of (6) with experimentally detected events can be seen on figure 3. The maximum geometrical height $H = |W_{mes} - W_{base}|_{max}$ of the response peak is then related to $A$ by the function

$$G(W_{base}, \tau_b) = H/A = (\tau_w/\tau_b)^{\frac{\tau_w}{\tau_b - \tau_w}}\ . \tag{7}$$

For say $W_{base} = 0.414$ Hz ($T = 129\ \mu$K) and $\tau_b = 5.0$ s, the slowing down

of the VWR response is hence responsible for the loss of 29 % of the signal amplitude.

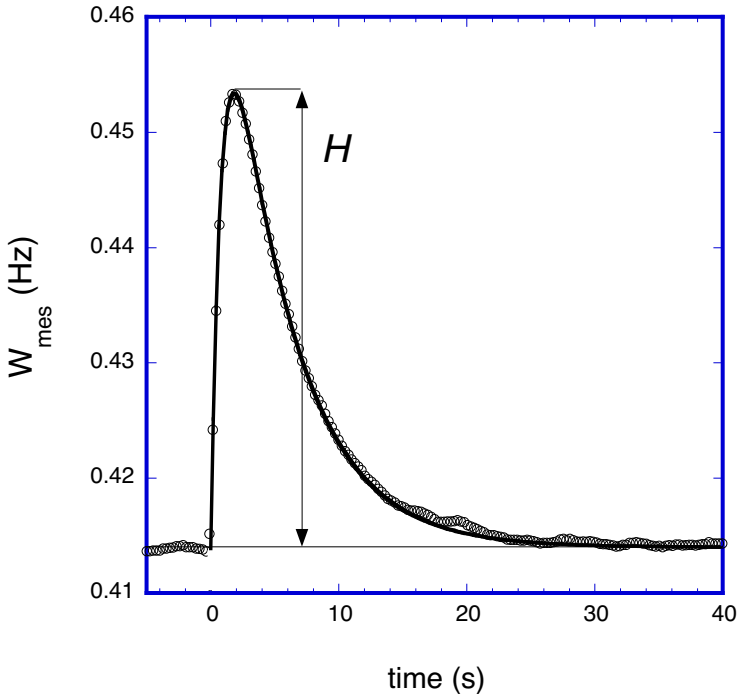


Fig. 3. Bolometrically recorded event ($\sim 100\,\mathrm{keV}$) (circles). The fit (line) by (6) uses the input parameters $W_{base} = 414\,\mathrm{mHz}$ and thus $\tau_w = 1/\pi W_{base}$ =0.77 s. The cell relaxation time $\tau_b = 5.0\,\mathrm{s}$ is fixed for all events of the entire experimental run. The only free parameters are the start time of the event and and $A$. Here the fit yields $A = 56.0\,\mathrm{mHz}$, in good consistency with $H \times G^{-1}(W_{base},\ \tau_b) = 55.4\,\mathrm{mHz}$.

## 4 Calibration factor

Both the enthalpy and $W_0$ are roughly proportional to the quasiparticle density. Therefore the bolometric calibration factor $\sigma$ of a given cell, defined as the conversion factor relating the amplitude $A$ ($\ll W_0$) of the rise in $W_0$ in

(5) to the heat $U$ released

$$\sigma = A/U, \tag{8}$$

is a slow function of temperature. Around 130 $\mu$K, the temperature dependence of the specific heat of $^3$He-B is given to a good approximation by [10,17]

$$C = C_0 \ (T_c/T)^{3/2} \ \exp(-\Delta/k_B T), \tag{9}$$

where $T_c$ is the superfluid transition temperature and $C_0 = 1.7$ mJ/Kcm$^3$. Writing $\delta U = CV\delta T$ allows to express the calibration factor using (1), (8) and (9) in the low velocity limit as

$$\sigma_0(T) = \frac{\alpha\Delta}{k_B C_0 V T_c^{3/2}} \ \frac{1}{\sqrt{T}}. \tag{10}$$

Taking into account the velocity dependence of the damping (2) leads to an enhancement of the calibration factor at higher velocities over $\sigma_0$ by a factor

$$f(u,t') = \sigma(v)/\sigma_0 = t' \left[ \left(1 + t'^{-1}\right) \frac{\sinh(u/2)}{u/2} - e^{-u/2} \right] \frac{\sinh(u/2)}{u/2}, \tag{11}$$

where $t' = k_B T/\Delta$ and $u = v/v_0$. At velocities $v \approx v_0$, this results consequently in an enhancement of the calibration factor by about 12 %. This analysis is valid for velocities up to $\sim 1.5\ v_0$, before the other dissipative mechanisms discussed set on.

Adding in (7) leads thus to the conclusion that the relation of the geometric height $H$ of a peak following a heat deposition $U$ depends on both the baseline $W_{base}$ and the $rms$ velocity $v$ of the oscillation following

$$H = \sigma_0 \; f(u, t') \times G(W_{base}, \tau_b) \times U. \tag{12}$$

## 5 Bolometric calibration by heater pulses

At ultra-low temperatures, simulation of heating events by Joule heating is inefficient in superfluid $^3$He because of the diverging thermal (Kapitza) resistance at the solid-liquid boundaries. Bradley *et al.* [3] proposed a heating method of the superfluid, based on the mechanical friction of the oscillating VWR with the liquid. Energy is injected through a second VWR present (the "heater" VWR, as in the lowest of the 3 cells in Fig. 1) by driving it over a short time with an excitation current at its resonance frequency. The energy is then dissipated to the superfluid via the velocity dependent frictional coupling. One should bare in mind that the electrically injected power is firstly transformed into mechanical energy of the resonator before being transfered to the liquid by friction. Therefore, even for a short excitation pulse of the heater ($\delta t \sim 100$ ms), the heat release to the liquid nevertheless takes place on a characteristic timescale given by (4), where the damping $W$ is relative to the heater wire.

The energy deposition by a heater pulse is hence not instantaneous, even in the case of extremely short pulses. We have estimated quantitatively this heat release, in order to verify wether a mechanical heater pulse is indeed an acceptable 'simulation' of a real - instantaneous - event. If one assumes velocity

independent damping of the heater resonator, its amplitude of oscillation must increase linearly during the pulse and then relax exponentially with timescale $\tau$. We have modeled numerically under these assumptions the heat release to the superfluid in such a heater pulse, as well as the response of the thermometer wire in the bolometric cell. One result and its comparison to the response calculated for an instantaneous energy release, as say by an incident particle, are given in Fig. 4. One can see that even though the shape of the thermometer's response is quite different, especially during the rise of the signal, the maximum amplitude is still the same within less than 1 % for $W_{base} > 0.3\,\mathrm{Hz}$. A fit of the response by (6) is therefore not appropriate in the case of mechanical heater pulses, while the geometrical maximum height $H$ of the response peak is still a good parameter for comparing pulses to instantaneous events.

A more serious issue for the bolometric calibration by mechanical heater pulses are the intrinsic losses within the heater wire. The intrinsic damping (i.e. in the absence of liquid) of a VWR can be well modelled by a viscous friction term which therefore simply adds as a constant extra term $W_{int}$ to the measured damping $W$ in (1). In our experiment, we measure the heater VWR intrinsic width as the limiting value of the damping in the low temperature limit, to be $W_{int}^{heater} = 77 \pm 6$ mHz. As the thermal quasiparticle damping vanishes at low temperatures, the intrinsic losses in the heater represent a fraction $W_{int}^{heater}/(W_{int}^{heater} + W_L^{heater})$ of the injected energy and constitute a non-negligible correction to the energy injection through the heater wire.

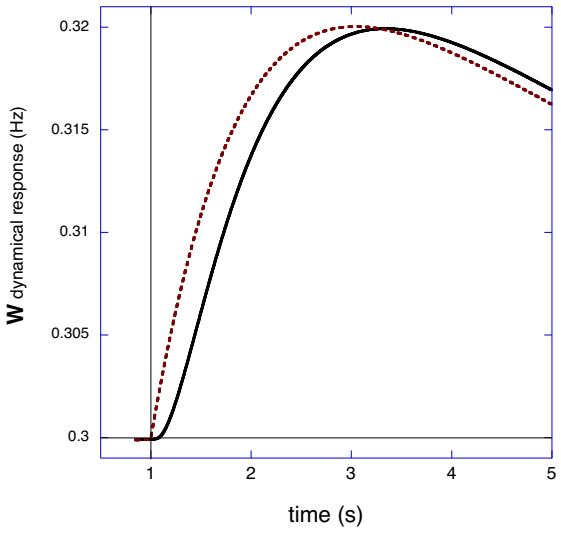


Fig. 4. Simulation of the response of the thermometer VWR to an instantaneous heat deposition at $t = 1$ s (dotted line) and to a mechanical heater pulse of same total energy but releasing the heat slowly (continuous line) because of $\tau_w^{heater}$. While the response to the instantaneous event is well described by (6), the response to the slow heat release has a different shape during the rise, but is then rather identical except for a time shift due to the slower release of the energy by the heater. The height $H$ of the two peaks is nevertheless identical within 1 % at 0.3 Hz (128 $\mu$K) and much less at higher temperatures.

Let us now consider the energy and velocity dependence of the detector response. At constant oscillation velocity, the height $H$ of the response is experimentally observed to be linear in the injected energy in the range of a few hundred keV (Fig. 5), which confirms the assumptions leading to (8). Furthermore, a comparison of the observed slopes versus the VWR's oscillation velocity (Fig. 6) are in good agreement with the enhancement of the response at higher velocities, as given by (11). This analysis allows therefore to extract the velocity independent limit of the calibration factor $\sigma_0$.

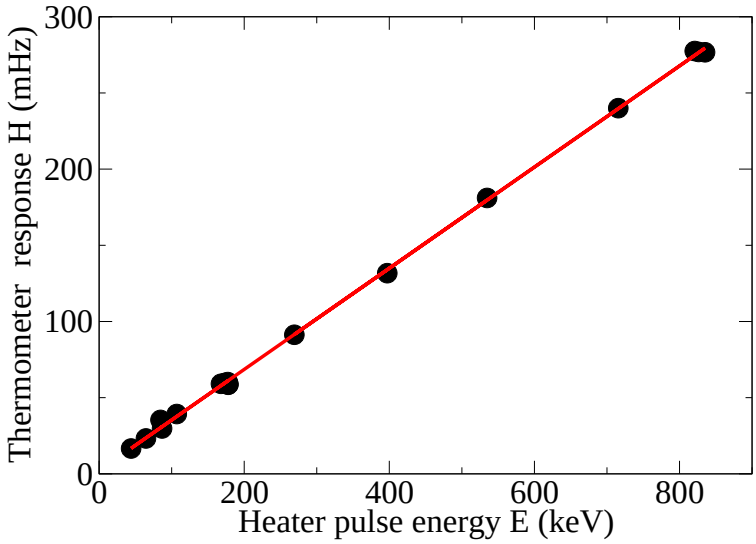


Fig. 5. Height $H$ of the response of the thermometer VWR to mechanical heater pulses of energy $E$ (bullets) and linear fit (data taken at $W_{base} = 1.7$ Hz).

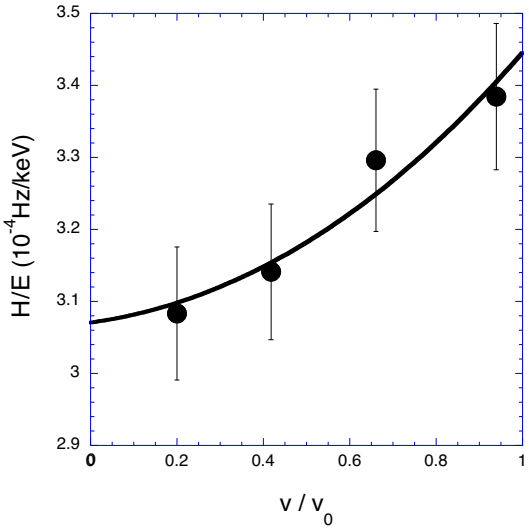


Fig. 6. Dependence of the observed slopes of $H(E)$ as in Fig. 5 as a function of the reduced oscillation velocity of the thermometer VWR ($W_{base} = 4$ Hz). The continuous line represents the expected evolution from (11), the only free parameter being $H/E(v = 0)$.

Taking into account intrinsic losses in the heater as well as the features of the thermometer VWR response deduced in the previous sections, one can fit the

mechanical pulse calibration data versus baseline (i.e. versus temperature) as shown in Fig. 7. If $W_{int}^{heater}$ is left as a free parameter, the fit yields a value of $W_{int}^{heater} = 74$ mHz and a calibration factor of $\sigma_0 = 3.8\ 10^{-4}$ Hz/keV at a baseline of 1 Hz (7). Imposing $W_{int}^{heater} = 77$ mHz leaves the overall prefactor of $\sigma_0$ (equivalent to the knowledge of $\alpha$) as the only free fitting parameter, with a value only 0.5% different.

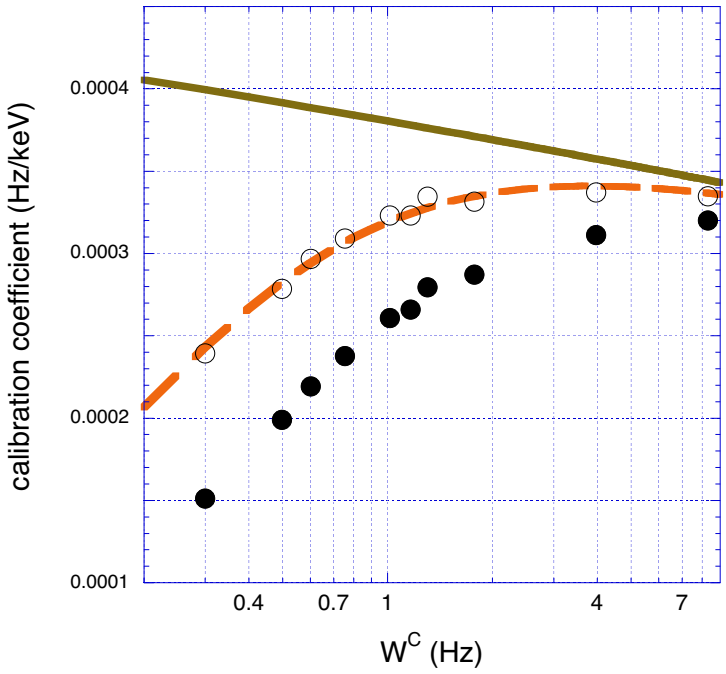


Fig. 7. Calibration of the observed H/E in the zero velocity limit from mechanical heater pulses (•). The data are then corrected by (7) to account for the slowing down of the thermometer at low temperatures (○). Considering the fact that a fraction $W_{int}^{heater}/W_{tot}^{heater}$ of the injected energy is dissipated inside the heater VWR, the result can be fitted by (10)(dashed line). The only free parameter is the overall prefactor of (10) which allows then to express $\sigma_0(T)$ (continuous line).

## 6 Neutrons

The heat release to the superfluid following a nuclear neutron capture reaction $^3\mathrm{He} + n \rightarrow {}^3\mathrm{H} + p$ was observed in [8] to be at 0 bar about 15 % less than the 764 keV known to be produced by the reaction. For a microscopic description of the stopping process of the neutron capture products in $^3$He we refer to [18]. A substantial part of the energy deficit can be attributed to ultra-violet (UV) scintillation [19]. The UV fraction was estimated in [8] to account for about half of the 15 % energy deficit, which led to the conclusion that the remaining approximately 60 keV were trapped in the form of topological defects.

Neutrons are an extremely valuable tool for the characterization of the superfluid bolometers because they provide a narrow and cell-geometry independent peak at rather high energies. Once the bolometric heat release of neutrons in $^3$He unambiguously determined, no other calibration, e.g. by pulses, is necessary. The comparison of the evolution of the observed neutron peak with temperature also allows to test directly, without the use of mechanical heater pulses, the assumptions leading to (12).

The dependence of the neutron peak position on the baseline (i.e. on temperature) is shown on Fig. 8. The agreement of the baseline dependence as given by (12) is good except for the very lowest temperatures where an absolute deviation from (12) of about 6 % is observed at $W_{base}$=100 mHz. The analysis yields a bolometric heat deposition of 652±23 keV at 0 bar, in very

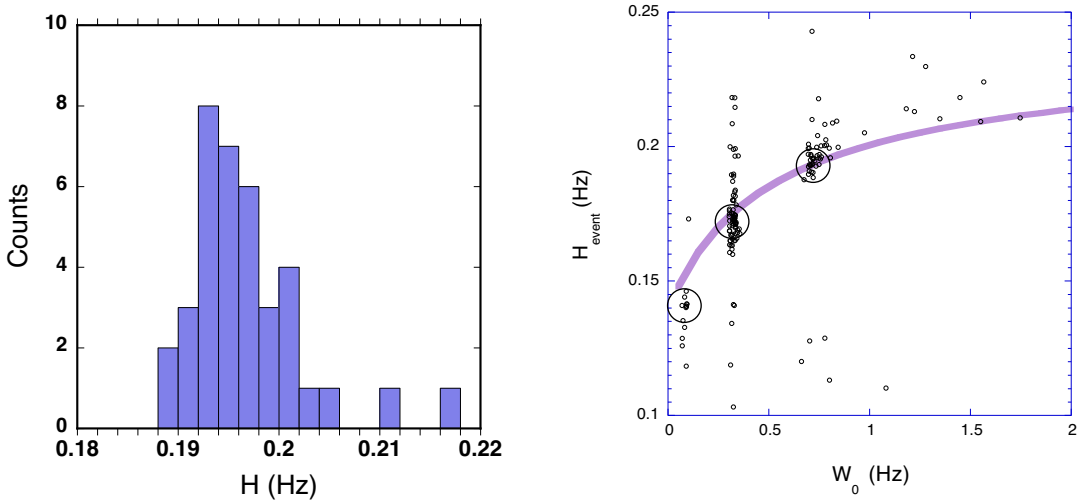


Fig. 8. Left: Constant baseline (0.71±0.03 Hz) histogram of detected events around the nuclear neutron capture peak at 0.194±0.004 Hz. The slight asymmetry of the peak can be attributed to superposition with low energy events, as well as to incident neutrons with non-negligible kinetic energies. Right: All detected events in the energy range of a few hundred keV in presence of the AmBe neutron source, as a function of $W_{base}$. Note that a large fraction of the points does not actually represent single neutron capture events and only the sites of larger concentration of events at a given $W_{base}$ (circles) correspond to the neutron peak at that temperature. The continuous line represents the temperature dependence of the expected height $H$ corresponding to the neutron peak, as given by (12).

good agreement with earlier measurements, where 650 keV were found under the same conditions [8]. Wether the observed energy deficit of about 110 keV can be significantly accounted for by topological defects is nevertheless still an open question. An extensive study of the pressure dependence of this deficit is in progress and might give some new insight on this question [20].

## 7 Scintillation yield in helium of muons and low energy electrons

The detection of electrons of mainly 7 and 14 keV emitted by a $^{57}$Co source within a single superfluid $^3$He-B bolometer has been reported recently [12]. The detected spectrum is consistent with the known emission spectrum of the source. However, an overall deficit of 23±7 % with respect to the bolometric calibration factor of that cell, determined as described in sections 2-5, is observed. Especially for ionizing events a significant energy release in the form of radiation is expected, producing a net deficit in the detected heat deposition. We therefore define the scintillation yield in the following as the fraction of the injected energy that is released as radiation.

In helium, the distance between two consecutive collisions of electrons in the keV range is a fraction of a $\mu$m. This distance is much larger than that in the case of $\alpha$-particles or the neutron capture products. Upon electron irradiation, the energy is hence deposited with much lower density and at no time the density of heat is such that the superfluid could heat up to the normal state. In the case of electrons, the energy deficit is therefore entirely due to UV scintillation. The scintillation yield is very sensitive to the density of the energy deposition. Our results can be compared to measurements by Adams *et al.* [21] who find a 35 % UV scintillation yield in $^4$He upon irradiation by electrons of a few hundred keV. Nevertheless, as later emphasized by McKinsey *et al.* [19,22], this measurement only covered the fast emission pulse of the first 10-

20 nanoseconds. A substantial part of the UV emission, estimated to about half of the fast pulse contribution by these authors, takes place at much later times, which brings the UV scintillation yield to a total of about 50 % for electrons of several hundred keV. At lower energies on the keV level, this fraction is expected to decrease rapidly. Our results concerning the scintillation rate of electrons around 10 keV represent thus a very reasonable low energy extension of the measurements by McKinsey *et al.*

The muon events also display in our detector a clearly resolved spectrum. Figure 9 shows data taken from [23], comparing numerical simulations to experimental results of the MACHe3 detector in the 10 to 200 keV range. A GEANT 4.0 code computer simulation of the muon energy release to the $^3$He cell, integrated over a large spectrum of incident muon energies, produces a broad peak at about 67 keV. The dispersion of the calculated energy distribution is a result of the muon tracks crossing the cell geometry in all space directions with the known angular dependence of radiation intensity [23]. The muon energy release to the target material is rather independent on the energy of the incident muons in the range from 1 to 10 GeV covering the maximum of the energy distribution of muons at ground level.

The width of the experimentally detected muon spectrum corresponds to the intrinsic resolution of our detector (3 %) combined to the geometrical broadening. The muons produce exclusively electron recoils in the cell, resulting in delta rays, i.e. electrons scattered from the atomic shells, energy-distributed

following $E_e^{-2}$. For one incident muon, roughly 10 of such electrons have an energy greater than 250 eV and only 5 greater than 1 keV.

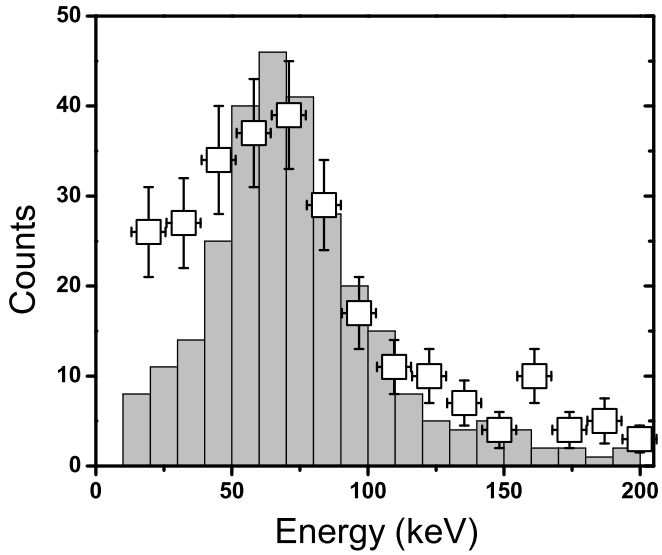


Fig. 9. Muon spectra: Scintillation-corrected experimental data (squares) and simulation (histogram) (data taken from [23]). Whereas the simulation estimates the *total energy* released by the muon flux to the detector, the bolometric measurements only detect the fraction converted to *heat*. By assuming a scintillated fraction of $x$=21 %, i.e. rescaling the experimentally detected muon peak by a factor $(1-x)^{-1}$, it can be well matched to the calculation. Non-muonic low energy events contribute to a broadening of the spectrum at lower energies.

In a previous experiment [23], data in the muon energy range were collected during 19 hours (Fig. 9). A broad maximum of events with an average energy matching the prediction is clearly seen. To obtain quantitative agreement of the two data sets, the experimental data were rescaled by a factor 1.27. We therefore again observe an energy deficit of the detected heat with respect to

the initial energy input, of about 21 % in the case of cosmic muons. The missing energy being the result of the scintillation of UV photons as for incident electrons, this observed deficit again allows to quantify the scintillation rate of helium for this type of irradiation.

Table 1

Measured energy release by different particles and their scintillation rates

| particle | cosmic muons | low energy electrons | $p$+$^3$H |
|---|---|---|---|
| initial kinetic energy (keV) | 2-4 $10^6$ | $13.6 \pm 0.8$ | 571+193 |
| energy release to target $^3$He (keV) | $< 67 > \pm 5$ | $13.6 \pm 0.8$ | 764 |
| bolometrical detection peak (keV) | $< 53 > \pm 5$ | $10.5 \pm 1$ | $652 \pm 23$ |
| scintillated fraction | $0.21 \pm 0.08$ | $0.23 \pm 0.07$ | $< 0.15 \pm 0.03$ |

## 8 Conclusions

We have presented a detailed description of the method of bolometric calibration of the detector cells based on superfluid $^3$He, by mechanical pulses. This description provides a general and comprehensive understanding of the bolometer under variable conditions of use (excitation level, temperature). The results of the calibration are compared to measured heat depositions by the nuclear neutron capture reaction as well as muon impacts and low energy electron irradiation. A deficit of about 15 % is found in the case of neutrons,

in good agreement with previous measurements at 0 bar [8], in which case this deficit is partly associated to vortex creation. In the case of cosmic muons as well as low energy electrons, a deficit in the 20 to 25 % range is found which can be entirely attributed to UV scintillation losses. It is not surprising to find the scintillation rates resulting from these two later types of irradiation to be similar since the much higher incident energy of cosmic muons is compensated by their larger mass. As the detector was recently demonstrated to display the required sensitivity for resolving recoils in the keV energy range [12], we have now focused on the the feasibility of an electron recoil rejection by parallel scintillation detection. Since we found the UV scintillation yield not to be small for both electrons and muons down to the energy range of interest, this result gives experimental evidence that the parallel use of a scintillation detector would allow to reject efficiently electron-, muon- and most likely $\gamma$-contamination in a bolometric detector based on superfluid $^3$He for the search of non-baryonic Dark Matter. The optimum design of such a parallel scintillation detector will be discussed in a future work.

The authors are grateful to the Région Rhône-Alpes and to the "Agence Nationale de la Recherche" (France) for providing financial support within the MACHe3 and ULTIMA projects. We also thank the European Science Foundation for supporting the COSLAB network workshops.

## References


[1] G. R. Pickett, in Proc. of the Second European workshop on neutrinos and dark matters detectors, ed. by L. Gonzales-Mestres and D. Perret-Gallix, Frontiers (1988), 377.

[2] Yu. M. Bunkov, S. N. Fisher, H. Godfrin, A. Guénault, and G. R. Pickett, in Proc. of International Workshop on Superconductivity and Particle Detection, ed. by T. Girard, A. Morales and G. Waysand, World Scientific (1995), 21-26.

[3] D. I. Bradley, Yu. M. Bunkov, D. J. Cousins, M. P. Enrico, S. N. Fisher, M. R. Follows, A. M. Guénault, W. M. Hayes, G. R. Pickett, and T. Sloan, Phys. Rev. Lett. **75** (1995) 1887.

[4] V. Sanglard *et al.*, Phys. Rev. **D71** (2005) 122002.

[5] D.S. Akerib *et al.*, Phys. Rev. Lett. **96** (2006) 011302.

[6] F. Mayet, D. Santos, G. Perrin, Yu. M. Bunkov, and H. Godfrin, Nucl. Instr. and Meth. **A455** (2000) 554.

[7] F. Mayet, D. Santos, Yu. M. Bunkov, E. Collin, and H. Godfrin, Phys. Lett. **B538** (2002) 257.

[8] C. Bäuerle, Yu. M. Bunkov, S. N. Fisher, H. Godfrin, and G. R. Pickett, Nature **382** (1996) 332.

[9] W. Zurek, Nature **317** (1985) 505.

[10] C. Bäuerle, Yu. M. Bunkov, S. N. Fisher, and H. Godfrin, Phys. Rev. **B57** (1998) 14381.

[11] C.B. Winkelmann, E. Moulin, Yu.M. Bunkov, J. Genevey, H. Godfrin, J. Macias-Pérez, J.A. Pinston, and D. Santos. "MACHE3, a prototype for non-baryonic dark matter search: KeV event detection and multicell correlation." In "Exporing the Universe, XXXIX Rencontres de Moriond", ed. Giraud-Heraud and Thanh Van, The Gioi (2004), 71.

[12] E. Moulin, C. Winkelmann, J.F. Macias-Pérez, Yu.M. Bunkov, H. Godfrin, D. Santos, Nucl. Instr. and Meth. **A548** (2005) 411.

[13] S. N. Fisher, A. M. Guénault, C. J. Kennedy, and G. R. Pickett, Phys. Rev. Lett. **63** (1989) 2566.

[14] C. B. Winkelmann, E. Collin, Yu. M. Bunkov, and H. Godfrin, J. Low Temp. Phys. **135** (2004) 3.

[15] S. N. Fisher, G. R. Pickett, and R. J. Watts-Tobin, J. Low Temp. Phys. **83** (1991) 225.

[16] D. I. Bradley, Phys. Rev. Lett. **84** (2000) 1252.

[17] D. Vollhardt and P. Wölfle, *The Superfluid Phases of Helium 3* Taylor & Francis (1990).

[18] J. S. Meyer and T. Sloan, J. Low Temp. Phys. **108** (1997) 345.

[19] D. N. McKinsey *et al.*, Phys. Rev.**A67** (2003) 62716.

[20] J. Elbs, C. B. Winkelmann, E. Collin, Yu. M. Bunkov, and H. Godfrin, in progress.

[21] J. S. Adams, Y. H. Kim, R. E. Lanou, H. J. Maris, and G. M. Seidel, J. Low Temp. Phys. **113** (1998) 1121.

[22] D. N. McKinsey *et al.*, Nucl. Instr. and Meth. **A516** (2004) 475.

[23] E. Moulin, Ph.D. Thesis, Université Joseph Fourier, 2005, unpublished.